Pharmaceutical Research, Vol. 25, No. 10, October 2008 (© 2008)
DOI: 10.1007/s11095-008-9632-1

Research Paper

Characterization of Substrates and Inhibitors for the *In Vitro* Assessment of Bcrp Mediated Drug–Drug Interactions

Uwe Muenster,[1] Birgit Grieshop,[1] Karsten Ickenroth,[1] and Mark Jean Gnoth[1,2]

Received February 29, 2008; accepted May 14, 2008; published online June 4, 2008

Purpose. *In vitro* assessment of drug candidates' affinity for multi-drug resistance proteins is of crucial importance for the prediction of *in vivo* pharmacokinetics and drug–drug interactions. To have well described experimental tools at hand, the objective of the study was to characterize substrates and inhibitors of Breast Cancer Resistance Protein (BCRP) and P-glycoprotein (P-gp).
Methods. Madin–Darbin canine kidney cells overexpressing mouse Bcrp (MDCKII-Bcrp) were incubated with various Bcrp substrates, or a mixture of substrate and inhibitor to either the apical (A) or basolateral (B) compartment of insert filter plates. Substrate concentrations in both compartments at time points $t = 0$ h and $t = 2$ h were determined by LC–MS/MS, and respective permeation coefficients (P_{app}) and efflux ratios were calculated.
Results. The Bcrp inhibitor Ko143 blocked topotecan and ABZSO transport in a concentration-dependent manner. P-gp inhibitors ivermectin, LY335979, PSC833, and the P-gp/Bcrp inhibitor ritonavir did not influence Bcrp mediated topotecan transport, however, blocked ABZSO transport. Additionally, neither was ABZSO transport influenced by topotecan, nor topotecan transport by ABZSO.
Conclusions. Data suggest different modes of substrate and inhibitor binding to Bcrp. In order to not overlook potential drug–drug interactions when testing drug candidates for inhibitory potential towards Bcrp, distinct Bcrp probe substrates should be used.

KEY WORDS: Bcrp; drug–drug interaction; inhibitor; pharmacokinetics; substrate.

INTRODUCTION

Multi-drug resistance proteins such as P-glycoprotein (P-gp, MDR1, ABCB1) and Breast Cancer Resistance Protein (BCRP, MXR, ABCP, ABCG2) play a crucial role in the absorption, distribution, and excretion of drugs (1). While their physiological role is to protect cells from toxic compounds, the extrusion of anti-cancer drugs from tumor cells leads to multi-drug resistance (2).

As opposed to the general structure of ABC transporters which usually comprises 12 transmembrane segments (*e.g.* true for P-gp), split into two halves, each with a nucleotide binding domain, BCRP is a so called half transporter (3). Various BCRP and P-gp residues being relevant for transport function were identified (3–5), the existence of multiple substrate binding sites in P-gp has been shown (6,7) and three-dimensional structures are available (8–10); yet the mechanism of transport is open to debate.

ABC transport proteins possess a broad range of substrate specificity, with many drugs being substrates or inhibitors of more than one transporter (11,12). For the assessment of whether or not a new chemical entity is a substrate for a certain drug transport protein, specific inhibitors as well as cell lines that overexpress respective transport proteins are fundamental tools. Ko143, a derivative of the natural compound Fumitremorgin C (13), was synthesized in order to improve both, affinity and specificity towards BCRP/Bcrp (14). With respect to P-gp, PSC833, LY335979 and ivermectin are routinely used inhibitors (15–17). However, knowledge of their effects on BCRP mediated drug transport is limited.

Drug–drug interactions resulting from inhibition of multi-drug resistance proteins are a clinical concern (18,19). Therefore FDA draft guideline not only demands determination of whether a drug candidate is a substrate, but also if it is an inhibitor of a certain transport protein (20). Up to four different binding sites have been speculated on P-gp (6,7), raising the question as to which substrate should be used to demonstrate the inhibitory potential of a new chemical entity (21).

In order to have well characterized experimental tools at hand, we utilized a flux assay using the Madin–Darbin canine kidney cell line MDCKII which overexpresses mouse BCRP

[1] Department of Metabolism and Pharmacokinetics, Bayer HealthCare AG, Aprather Weg, 42096, Wuppertal-Aprath, Germany.
[2] To whom correspondence should be addressed. (e-mail: markjean.gnoth@bayerhealthcare.com)

ABBREVIATIONS: A, apical; ABCB1, ATP binding cassette transporter B1; ABCG2, ATP binding cassette transporter G2; ABCP, human placenta-specific ATP-binding cassette gene; ABZSO, albendazole sulphoxide; B, basolateral; BCRP, breast cancer resistance protein; DMEM, Dulbecco's modified Eagle's medium; DMSO, dimethylsulfoxide; FCS, fetal calf serum; HBSS, Hanks' balanced salt solution; HEPES, 4-(2-hydroxyethyl)-1-piperazineethanesulfonic acid); LLC-PK1, porcine kidney tubular epithelial cell line; MDCKII, Madin Darby canine kidney cell line II; MXR, mitoxantrone resistance gene; P_{app}, apparent permeability coefficient; P-gp, P-glycoprotein; TEER, transepithelial electrical resistance; wt, wild-type.

(Bcrp) (22). Transport interactions of the Bcrp substrates topotecan (22), albendazole sulphoxide (ABZSO) (23), imatinib (24), and prazosin (25) as well as their interaction with various P-gp- and Bcrp inhibitors including Ko143, PSC833, LY335979, ivermectin, and ritonavir (26) were determined.

METHODS AND MATERIALS

Chemicals. Albendazole sulphoxide (ABZSO) was purchased from ABCR (Karlsruhe, Germany); topotecan from LKT Laboratories Inc. (St. Paul, MI); ivermectin, dipyridamole, prazosin, vincristine, dimethylsulfoxide (DMSO), glucose, and ammonium acetate from Sigma (Taufkirchen, Germany); acetonitrile from Merck (Darmstadt, Germany); 4-(2-hydroxyethyl)-1-piperazineethanesulfonic acid (HEPES), fetal calf serum (FCS), Hanks' balanced salt solution (HBSS), Dulbecco's modified Eagle's medium (DMEM), Medium 199, glutamine, trypsin, penicillin, and streptomycin from Gibco Life Technologies (Eggenheim, Germany); Ko143, PSC833, ritonavir, and LY335979 were synthesized at Bayer Healthcare chemical laboratories (Wuppertal, Germany).

Cell culture. MDCKII-wt, MDCKII-Bcrp cells (22), and a porcine kidney tubular epithelial cell line (LLC-PK1) (27) overexpressing MDR1 (L-MDR1) were purchased from the Netherlands Cancer Institute, Amsterdam. MDCKII cells were grown in DMEM supplemented with 10% FCS, 10,000 IU/500 mL penicillin, and 10 mg/500 mL streptomycin (MDCKII growth medium), and cultured at 8% CO_2. L-MDR1 cells grown in Medium 199, and supplemented with 10% FCS, 10,000 IU/500 mL penicillin, 10 mg/500 mL streptomycin, 0.59 μg/mL vincristine, and 2 mM glutamine (L-MDR1 growth medium), were cultured at 5% CO_2.

Flux assay. With MDCKII cells, 2.5×10^5 cells were seeded into 24-well microporous insert filter plates (0.4 μm pore diameter, Corning Star Corporations, Cambridge, USA) and cultured in growth medium for 4 days with one media change on day 3. On day 4 medium was replaced with HBSS containing 5 mM HEPES and 20 mM glucose (transport buffer). After a 20 min incubation period at 37°C, the assay was started by aspirating the transport buffer and subsequent addition of the respective substrate, or a mixture of substrate and inhibitor (dissolved in HBSS containing 5 mM HEPES, 20 mM glucose, and 1% DMSO) to either the apical (A) or basolateral (B) compartment of the 24-well insert filter plates for 2 h at 37°C. With L-MDR1 cells, 2×10^5 cells were seeded into 96-well insert filter plates (0.4 μm pore diameter, Corning Star Corporations, Cambridge, USA). Assay conditions were the same as for MDCKII cells, except that L-MDR1 transport buffer did not contain glucose. Substrate concentrations in both compartments at time points $t = 0$ h and $t = 2$ h were determined by LC–MS/MS.

Liquid chromatography was performed on an Agilent 1100 liquid chromatography system (Cohesive Technologies, Aschaffenbug, Germany) equipped with a Phenomenex Aqua C18 column (150 × 2 mm, 5 μm particle size; Phenomenex, Aschaffenburg, Germany; used for topotecan, prazosin, and ABZSO), or a Purospher Star C18 column (4 × 55, 3 μm particle size; Merck, Darmstadt, Germany; used for imatinib) at a flow rate of 0.5 mL/min. The mobile phase consisted of two solvents: for topotecan, prazosin, and ABZSO, a 10 mM ammonium acetate buffer pH 3 (A), and acetonitrile (B) were used. For imatinib, a 10 mM ammonium acetate buffer pH 6.8 (A), and acetonitrile (B) were used. The gradient profiles were: topotecan: 0 to 0.5 min, 5% B; 0.5 to 1.5 min, linear gradient to 90% B; 1.5 to 3.0 min, 90% B; 3.0 to 3.2 min, linear gradient to 5% B, 3.2 to 5 min, 5% B. ABZSO: 0 to 1.0 min, 10% B; 1.0 to 2.0 min, linear gradient to 90% B; 2.0 to 4.0 min, 90% B; 4.0 to 4.2 min, linear gradient to 10% B; 4.2 to 5.0 min, 10% B. prazosin: 0 to 1.0 min, 10% B; 1.0 to 2.0 min, linear gradient to 80% B; 2.0 to 3.5 min 80% B; 3.5 to 4.0 min, linear gradient to 10% B; 4.0 to 5.0 min, 10% B. imatinib: 0 to 0.5 min, 5% B; 0.5 to 1.5 min, linear gradient to 90% B; 1.5 to 3.0 min, 90% B; 3.0 to 3.2 min, linear gradient to 5% B, 3.2 to 5 min, 5% B. Mass spectrometry was performed on an ABI 3000 mass spectrometer (Applied Biosystems, Darmstadt, Germany) equipped with a turbo ion spray source for electrospray ionization. Samples were analyzed with positive polarity, key instrumental conditions were optimized to yield best sensitivity.

In preliminary experiments concentrations of substrates were determined using external calibration standards (LOQ's for topotecan, imatinib, prazosin, and ABZSO were approximately 1 ng/mL). However, similar data were obtained when peak areas were used directly for the calculation of P_{app} values and efflux ratios.

Therefore, respective permeability coefficients (P_{app}) and efflux ratios were calculated using the following equations:

1) P_{app} [cm/s] = (LC–MS/MS peak area of substrate in acceptor compartment at end of incubation × volume of medium in acceptor compartment [cm^3]) / (incubation time [s] × membrane surface area [cm^2] × LC–MS/MS peak area of substrate in donor compartment at start of incubation)
2) Efflux ratio = P_{app} B-A / P_{app} A-B

To ensure confluence of the MDCKII cell monolayer in each well, transepithelial electrical resistance (TEER) was measured at $t = 0$ h and $t = 2$ h between apical and basolateral compartment. With L-MDR1 cells, Lucifer Yellow was added to each well at time point $t = 0$ h, and its permeation measured by fluorimetry served as a marker of cell monolayer integrity (28).

Statistics. Each value given in tables and figures represents the mean result of three individual wells. Wilcoxon test was used where applicable. Inhibition curves and IC_{50} values were generated using Sigma Plot 8.0 (SPSS, Chicaco, USA).

RESULTS

Cells were used at passages seven to 26 after thawing. No significant passage dependent change in transport activity was observed (data not shown). Throughout all experiments with MDCKII-Bcrp cells, TEER values ranged between 250 and 450 $\Omega \times cm^2$. Within each experiment there were no hints on toxic effects of added compounds on MDCKII-Bcrp and L-MDR1 cells, since TEER at $t = 0$ h and $t = 2$ h showed no

significant changes, and the amount of permeated Lucifer Yellow was always below 1% (*n*/*n*)/h, respectively.

Transport in MDCKII Wild-type Cells

In order to assess the basal level of substrate transport in MDCKII-Bcrp cells by proteins other than overexpressed Bcrp, topotecan, ABZSO, prazosin, and imatinib (all at 2 μM) transport in MDCKII-wt cells was determined. With topotecan, P_{app} A-B, P_{app} B-A, and efflux ratios (P_{app} B-A/P_{app} A-B) ranged from 1.6 ± 0.0 to 2.5 ± 0.5 × 10^{-6}cm/s, 4.9 ± 0.4 to 7.3 ± 1.0 × 10^{-6}cm/s, and 2 to 3.7 indicating weak topotecan transport. With ABZSO, no significant transport was observed in MDCKII-wt cells (P_{app} B-A, 19.8 ± 10.9 × 10^{-6}cm/s; P_{app} A-B, 27.8 ± 5.3 × 10^{-6}cm/s; efflux ratio, 0.7; n = 3, mean±SD). The same was true for prazosin (P_{app} B-A, 26.0 ± 2.6 × 10^{-6}cm/s; P_{app} A-B, 44.6 ± 5.3 × 10^{-6}cm/s; efflux ratio, 0.6; n = 3, mean±SD) and imatinib (P_{app} B-A, 18.9 ± 4.4 × 10^{-6}cm/s; P_{app} A-B, 20.8 ± 1.5 × 10^{-6}cm/s; efflux ratio, 0.9; n = 3, mean±SD).

Transport in MDCKII-Bcrp Cells

When MDCKII-Bcrp cells were incubated with increasing concentrations of topotecan and ABZSO, transport efficiency in MDCKII-Bcrp cells was not significantly altered up to concentrations of 500 μM (Table I). With topotecan, P_{app} B-A, P_{app} A-B, and efflux ratios ranged from 7.5 ± 0.5 × 10^{-6} to 12.3 ± 0.4 × 10^{-6}cm/s, 0.5 ± 0.1 × 10^{-6} to 1.0 ± 0.1 × 10^{-6}cm/s, and 10.2 to 15.9, respectively. As for ABZSO, P_{app} B-A, P_{app} A-B, and efflux ratios ranged from 43.2 ± 4.1 × 10^{-6} to 56.9 ± 2.7 × 10^{-6}cm/s, 5.8 ± 0.0 × 10^{-6} to 6.2 ± 1.2 × 10^{-6}cm/s, and 7.4 to 9.3, respectively. In contrast, imatinib efflux ratios decreased in a concentration-dependent manner, indicating transport saturation starting at concentrations of about 10 μM (Table I). As for prazosin, transport saturation occurred at a concentration of 100 μM, if at all (Table I). For further inhibition experiments substrates were used at a concentration of 1 μM (imatinib, prazosin) or 2 μM (topotecan, ABZSO).

Influence of Ko143 on Bcrp Mediated Transport

Ko143, a specific inhibitor of BCRP/Bcrp (14) strongly decreased topotecan transport resulting in a reduction of efflux ratios from 19.3 without inhibitor, down to 1.5 in the presence of 5 μM Ko143 (IC_{50}, 0.12 ± 0.02 μM; Fig. 1A). A similar result was obtained for ABZSO (2 μM) transport in the presence of increasing concentrations of Ko143 (IC_{50}, 0.04 ± 0.004 μM; Fig. 1A). Also Bcrp mediated prazosin and imatinib transport were completely blocked by 5 μM Ko143 (Table II), which is reflected by a decrease of prazosin and imatinib efflux ratios down to 5.2% and 2.8% of control efflux ratios (referred to as 100%), respectively.

Influence of PSC833, LY335979, Ivermectin, and Ritonavir on Bcrp Mediated Transport

When MDCKII-Bcrp cells were incubated with the P-gp inhibitors PSC833, LY335979, ivermectin, and the P-gp/Bcrp inhibitor ritonavir (up to 100 μM), topotecan transport was not affected (Fig. 1B, Table II). In contrast, ivermectin, LY335979, PSC833, and ritonavir inhibited Bcrp mediated ABZSO transport. IC_{50} values for ivermectin, LY335979, and ritonavir mediated Bcrp inhibition were 2.2 ± 0.19, 7.8 ± 0.68, and 10.5 ± 1.5 μM respectively (Fig. 1B, Table II; IC_{50} value for PSC833 were not determined). Furthermore, the influence of ivermectin and ritonavir on imatinib and prazosin transport was investigated. Both, ivermectin and ritonavir blocked

Table I. Concentration Dependency of Topotecan and ABZSO Transport in MDCKII-Bcrp Cells

	P_{app} B-A [10^{-6}cm/s]	P_{app} A-B [10^{-6}cm/s]	Efflux ratio
Conc. topotecan [μM]			
0.5	12.3 ± 0.4	0.8 ± 0.1	15.4
2	11.7 ± 2.2	0.7 ± 0.1	15.9
50	10.0 ± 1.8	1.0 ± 0.1	10.2
500	7.5 ± 0.5	0.5 ± 0.1	13.7
Conc. ABZSO [μM]			
0.4	53.8 ± 3.6	6.2 ± 1.2	8.7
2	53.8 ± 5.9	5.9 ± 0.9	9.1
100	56.9 ± 2.7	6.1 ± 0.7	9.3
500	43.2 ± 4.1	5.8 ± 0.0	7.4
Conc. imatinib [μM]			
1	58.6 ± 3.1	2.7 ± 0.4	22.1
2	52.8 ± 3.6	1.8 ± 0.1	28.9
10	51.9 ± 5.0	5.8 ± 2.5*	9.0
100	22.1 ± 2.8*	8.3 ± 1.1*	2.7
Conc. prazosin [μM]			
1	70.8 ± 11.0	2.3 ± 0.1	30.4
2	59.0 ± 4.2	1.7 ± 0.1	35.5
10	75.3 ± 7.0	2.2 ± 0.0	34.7
100	64.4 ± 6.5	3.4 ± 0.1*	19.0

MDCKII-Bcrp cells were incubated with topotecan (0.5–500 μM), ABZSO (0.4–500 μM), imatinib (1–100 μM), or prazosin (1–100 μM) as described in "METHODS AND MATERIALS". P_{app} values and efflux ratios were calculated. Each value given represents the mean result of three individual wells (n=3, mean±SD). The experiment was repeated once, similar results were obtained.
*P=0.05; Wilcoxon

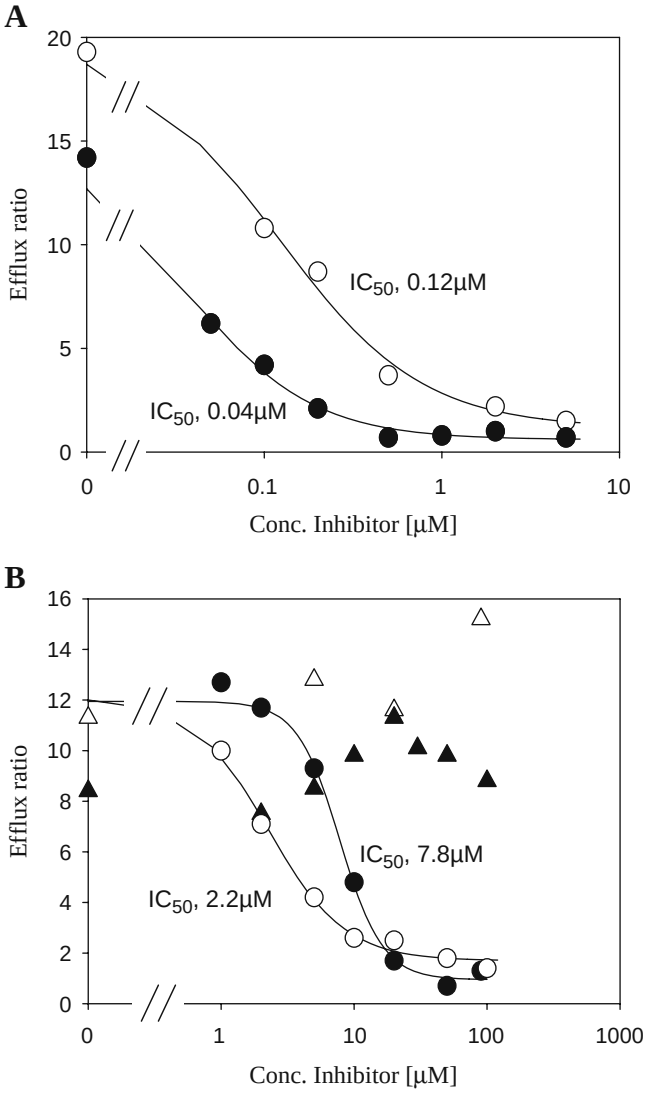

Fig. 1. Effects of Ko143 (**A**), as well as ivermectin and LY335979 (**B**) on Bcrp mediated topotecan and ABZSO transport. MDCKII-Bcrp cells were incubated with 2 μM topotecan or ABZSO 2 μM, in the presence of increasing concentrations of Ko143, LY335979, and ivermectin as described in "METHODS AND MATERIALS". Respective efflux ratios were calculated. **A** *Open circles*, topotecan efflux ratios; *closed circles*, ABZSO efflux ratios. **B** *Open circles*, ABZSO efflux ratios in the presence of ivermectin; *closed circles*, ABZSO efflux ratios in the presence of LY335979; *open triangles*, topotecan efflux ratios in the presence of ivermectin; *closed triangles*, topotecan efflux ratios in the presence of LY335979. Each point in the curves represents the mean efflux ratio (P_{app} B-A/P_{app} A-B) derived from P_{app} values of three individual wells for P_{app} B-A and P_{app} A-B, respectively. The experiment was repeated twice and showed similar results.

imatinib transport, and, to a lesser extent, prazosin transport as well (Table II).

Influence of PSC833, LY335979, and Ivermectin on P-gp Mediated Transport

In parallel, ivermectin, LY335979, and PSC833 exhibited a strong inhibition of P-gp mediated transport of 1 μM dipyridamole, a strong P-gp substrate (29), in L-MDR1 cells (IC_{50} for ivermectin, 0.42 ± 0.01 μM; IC_{50} for LY335979, 0.38 ± 0.01 μM; IC_{50} for PSC833, 0.078 ± 0.001 μM; graphs not shown).

Substrate–substrate Interactions

To further shed light on the fact that Bcrp mediated topotecan transport was not influenced by ivermectin, LY335979, PSC833, and ritonavir (Fig. 1B, Table II), whereas in contrast ABZSO transport was inhibited, the influence of topotecan on Bcrp mediated ABZSO transport, and *vice versa* was investigated. Indeed, neither was ABZSO transport influenced by 20 μM topotecan, nor topotecan transport by 100 μM ABZSO (Tables II and III). Looking further at substrate/substrate interactions, imatinib blocked Bcrp mediated transport of topotecan, ABZSO, and prazosin (Table II). The other way round, imatinib transport was neither influenced by 20 μM topotecan nor a 100 μM ABZSO (Table II). Also 20 μM topotecan and 100 μM ABZSO together had no influence on Bcrp mediated imatinib transport (data not shown).

Prazosin, at a concentration of 100 μM, blocked ABZSO, imatinib and topotecan transport, however, only partially (Table II). When looking at prazosin as a substrate, prazosin transport was not influenced by 20 μM topotecan. In contrast, ABZSO at 100 μM inhibited prazosin transport, resulting in a decrease of prazosin efflux ratio down to 46.9% of control efflux ratio (referred to as 100%) (Table II).

DISCUSSION

Recent publications have demonstrated that multidrug resistance transport proteins, *e.g.* P-gp and Bcrp, play a critical role in clinically observed pharmacokinetic interactions (18,19). The first step to avoid such interactions is to assess whether or not a new chemical entity is a substrate or inhibitor of transport proteins. This requires cell lines which overexpress respective transport protein as well as specific inhibitors. Then, with respect to proving that a new drug candidate is not an inhibitor of a transport protein, the following question comes up: Which substrate is going to be used to assess the inhibitory potential of a drug candidate? Because multiple drug binding sites have been shown to exist in P-gp (6,7), inhibitory effects on one binding site may be overlooked by choosing a substrate which binds to the other. Therefore, in order to address these issues with regard to Bcrp, we describe Bcrp substrate/substrate and substrate/inhibitor interactions using an *in vitro* flux assay.

As expected from previous data, topotecan (22), ABZSO (23), imatinib (24), and prazosin (25) were transported by MDCKII-Bcrp cells (Table I). Bcrp mediated topotecan and ABZSO transport were not saturated up to concentrations of 500 μM, suggesting that both drugs are low affinity/high capacity substrates for Bcrp. The same appeared to be true for prazosin since transport was saturated only with 100 μM prazosin, if at all (though concentrations between 10 and 100 μM were not tested). In contrast, saturation of Bcrp mediated imatinib transport started at 10 μM, which is in line with previous data (25).

The observed IC_{50} for the inhibition of Bcrp mediated substrate transport by Ko143 (Fig. 1A) is in accordance with

Table II. Inhibitory Effects of Drugs on the Efflux Ratio of Bcrp Substrates in MDCKII-Bcrp Cells Displayed as Percent of Control or IC_{50}

	Substrate			
Inhibitor	Topotecan	ABSZO	Imatinib	Prazosin
KO143	0.12 μM (IC_{50})	0.04 μM (IC_{50})	5.2% (5 μM)	2.8% (5 μM)
Ivermectin	n.e. (100 μM)	2.2 μM (IC_{50})	1.4% (10 μM)	40.9% (10 μM)
LY335979	n.e. (100 μM)	7.8 μM (IC_{50})	n.d.	n.d.
PSC833	n.e. (100 μM)	17.8% (10 μM)	n.d.	n.d.
Ritonavir	n.e. (100 μM)	10.5 μM (IC_{50})	9.8% (100 μM)	21.4% (100 μM)
Topotecan		n.e. (20 μM)	n.e. (20 μM)	n.e. (20 μM)
ABSZO	n.e. (100 μM)		n.e. (20 μM)	46.9% (100 μM)
Imatinib	17.5%(100 μM)	11.5 μM (IC_{50})		1.6% (100 μM)
Prazosin	44.6% (100 μM)	33.9% (100 μM)	30.9% (100 μM)	

MDCKII-Bcrp cells were incubated with substrate, with or without inhibitor as described in "METHODS AND MATERIALS". P_{app} A-B and P_{app} B-A values and efflux ratios were calculated. Numbers given represent percent of control based on the efflux ratio without inhibitor. Inhibitor concentrations are given in brackets; IC_{50} values are given where determined (refer also to Fig. 1A and B). Substrate concentrations used were 1 μM (imatinib, prazosin) and 2 μM (topotecan and ABZSO).
n.d. not determined, *n.e.* no effect on the efflux ratio observed

data previously obtained when inhibition of intracellular mitoxantrone accumulation by Ko143 was shown in drug resistant mouse MEF3.8/T6400 and human IGROV/T8 cells (14). The mode of Ko143 binding to Bcrp, to our knowledge, has not yet been fully clarified. However, it has been shown that Ko143 binding to human BCRP brings a conformational change that is different from substrate binding to the protein (30). Because in our experiments Ko143 blocked efflux of topotecan, ABZSO, imatinib and prazosin, the induction of a crucial conformational change of the Bcrp dimer, and therefore an allosteric mode of inhibition, is more likely than a competitive mechanism. It has to be taken into account that the IC_{50} for topotecan might be biased by the fact that topotecan showed a weak transport in wild type MDCKII cells. However, with regard to the efflux ratios in the transfected and wild type cells this effect should be of minor relevance, if at all.

The P-gp inhibitors PSC833, LY335979, and ivermectin unexpectedly blocked ABZSO transport. In parallel, we demonstrated that ABZSO is not a P-gp substrate using L-MDR1 cells (efflux ratio, 0.7, data not shown), and that ABZSO was not transported in MDCKII-wt cells (see "RESULTS" section). These findings are in line with a previous publication demonstrating that ABZSO is not a substrate for P-gp (23). Taken together, one can exclude that the observed inhibition of ABZSO transport in MDCKII-Bcrp cells by ivermectin, LY335979, and PSC833 was P-gp mediated transport. Therefore, ivermectin, LY335979, and PCS833 indeed inhibited Bcrp mediated transport of ABZSO. Also ritonavir, a known P-gp/Bcrp inhibitor (26) blocked Bcrp mediated ABZSO transport.

Interestingly, comparison of ivermectin, LY335979, and PSC833 effects on Bcrp mediated transport inhibition, with those on P-gp mediated dipyridamole transport inhibition, hints that ivermectin, LY335979, and PSC833 are relatively potent P-gp-, and rather weak Bcrp-inhibitors. Therefore, the concentration at which these three inhibitors are used in a transport assay may differentiate between P-gp and Bcrp inhibition.

Strangely, while decreasing Bcrp mediated ABZSO transport, all four inhibitors (PSC833, LY335979, ivermectin, and ritonavir) did not inhibit topotecan transport, suggesting different modes of substrate and inhibitor binding to Bcrp. This theory is underlined by the fact that topotecan and ABZSO did not interact with each other's transport, indicating separate substrate binding sites in Bcrp.

Recently strong evidence for the existence of at least two separate binding sites in the R482G BCRP mutant has been presented (31). It was shown that daunomycin was displaced from plasma membranes of BCRP overexpressing insect cells

Table III. Influence of ABZSO on Topotecan Transport, and of Topotecan on ABZSO Transport

Substrate (2 μM)	Inhibitor	P_{app} B-A [10^{-6} cm/s]	P_{app} A-B [10^{-6} cm/s]	Efflux ratio
ABZSO	–	33.9±3.4	2.3±0.4	14.7
ABZSO	Topotecan (5 μM)	34.3±2.6	2.3±0.3	14.9
ABZSO	Topotecan (20 μM)	38.6±13.5	2.8±0.1	13.8
Topotecan	–	6.7±1.5	0.6±0.1	11.2
Topotecan	ABZSO (5 μM)	6.6±2.0	0.6±0.1	11.0
Topotecan	ABZSO (100 μM)	11.0±0.2	0.9±0.1	12.2

MDCKII-Bcrp cells were incubated with 2 μM topotecan, with or without ABZSO at indicated concentrations; and with 2 μM ABZSO, with or without topotecan at indicated concentrations as described in "METHODS AND MATERIALS". Respective P_{app} values and efflux ratios were calculated. Each value given represents the mean result of three individual wells (n=3, mean±SD). The experiment was repeated twice and showed similar results.

to a varying extent, depending on the substrate used. *E.g.* partial displacement by mitoxantrone and Hoechst33342 was interpreted as daunomycin binding to two separate binding sites, and that mitoxantrone as well as Hoechst33342 displace from one, but not the other. Also Nakanishi *et al.* speculated a complex interaction of substrate with the BCRP transport protein (WT-BCRP and R482T variant), since in their substrate interaction studies using Rhodamin 123, topotecan, mitoxantrone, and flavopiridol, no two substrates reciprocally inhibited the efflux of the other (32).

In our investigations, imatinib inhibited transport of topotecan and ABZSO, however, reciprocal inhibition of imatinib transport by either ABZSO or topotecan alone, or both in combination, did not take place. This may be due to imatinib's higher affinity towards Bcrp, when compared to topotecan and ABZSO. Another explanation may be an allosterical mode of imatinib binding to Bcrp, in a way that imatinib efflux is being accompanied by a conformational change of Bcrp subunits which in turn prohibits topotecan and ABZSO transport. Or even, that there are two separate binding sites for imatinib, a high affinity binding site for its efflux, and a low affinity binding site contributing to a conformational change upon imatinib binding. If this would be true, the observed imatinib transport "saturation" that was observed at concentrations >10 μM could be in fact inhibition of imatinib transport by itself. However, there is no proof of this theory since we did not determine K_{on}/K_{off} rates for substrate binding to Bcrp. Another consideration is, that recently, it was shown that imatinib decreased the expression of BCRP in the BCR-ABL expressing cell line K562/BCRP-MX10 via downregulation of the Phosphoinositol-3-kinase (PI3K)/Akt pathway, whereas this effect was not observed in cells that do not express BCR-ABL (33). To our knowledge the expression of a BCR-ABL canine homologue in MDCKII-Bcrp cells has not been shown, however, a reduction of Bcrp mediated transport in MDCKII-Bcrp cells via PI3K/Act pathway downregulation in the presence of imatinib cannot be fully excluded.

Also with prazosin, distinct substrate–substrate interactions occurred (*e.g.* prazosin transport was inhibited by imatinib, but not by topotecan), underlining the hypothesis of different modes of substrate and/or inhibitor binding to Bcrp.

Taken together, P-gp inhibitors PSC833, LY335979, and ivermectin can block Bcrp mediated substrate efflux. The fact that all four inhibitors only blocked ABZSO, but not topotecan transport, and at the same time topotecan and ABZSO were unable to interact with each others transport, hints that physically separate binding sites for different substrates and inhibitors may be present in Bcrp, as it was shown for P-gp (6,7).

Considering drug–drug interactions, this is of importance because not all Bcrp substrates will interact with each other. Therefore, Bcrp substrates that are intended for co-administration, should be individually tested *in vitro* using the supposed co-administered drug as substrate, and *vice versa*.

ACKNOWLEDGEMENTS

We thank Mark Twele for technical assistance during LC–MS/MS analytics.

REFERENCES

1. Y. Shitara, T. Horie, and Y. Sugiyama. Transporters as a determinant of drug clearance and tissue distribution. *Eur. J. Pharm. Sci.* **27**:425–446 (2006).
2. F. Staud and P. Pavek. Breast cancer resistance protein (BCRP/ABCG2). *Int. J. Biochem. Cell Biol.* **37**:720–725 (2005).
3. P. Krishnamurthy and J. D. Schuetz. Role of ABCG2/BCRP in biology and medicine. *Annu. Rev. Pharmacol. Toxicol.* **46**:381–410 (2006).
4. J. D. Allen, S. C. Jackson, and A. H. Schinkel. A mutation hot spot in the Bcrp1 (Abcg2) multidrug transporter in mouse cell lines selected for doxorubicin resistance. *Cancer Res.* **62**:2294–2299 (2002).
5. T. W. Loo and D. M. Clarke. Identification of residues within the drug-binding domain of the human multidrug resistance P-glycoprotein by cysteine-scanning mutagenesis and reaction with dibromobimane. *J. Biol. Chem.* **274**:35388–35392 (2002).
6. A. B. Shapiro, K. Fox, P. Lam, and V. Ling. Stimulation of P-glycoprotein-mediated drug transport by prazosin and progesterone; evidence for a third drug binding site. *Eur. J. Biochem.* **259**:841–850 (1999).
7. C. Martin, G. Berridge, C. F. Higgins, P. Mistry, P. Charlton, and R. Callaghan. Communication between multiple drug binding sites on P-glycoprotein. *Mol. Pharmacol.* **58**:624–632 (2000).
8. R. J. Dawson and K. P. Locher. Structure of a bacterial multidrug ABC transporter. *Nature* **443**:180–185 (2006).
9. M. F. Rosenberg, R. Callaghan, S. Modok, C. F. Higgins, and R. C. Ford. Three-dimensional structure of P-glycoprotein—the transmembrane regions adopt an asymmetric configuration in the nucleotide-bound state. *J. Biol. Chem.* **280**:2857–2862 (2005).
10. J. Y. Lee, I. L. Urbatsch, A. E. Senior, and S. Wilkens. Projection structure of P-glycoprotein by electron microscopy—evidence for a closed conformation of the nucleotide binding domains. *J. Biol. Chem.* **277**:40125–40131 (2002).
11. L. M. Chan, S. Lowes, and B. H. Hirst. The ABCs of drug transport in intestine and liver: efflux proteins limiting drug absorption and bioavailability. *Eur. J. Pharm. Sci.* **21**:25–51 (2004).
12. E. Petzinger and J. Geyer. Drug transporters in pharmacokinetics. *Naunyn-Schmiedeberg's Arch. Pharmacol.* **372**:465–475 (2006).
13. C. B. Cui, H. Kakeya, and H. Osada. Novel mammalian cell cycle inhibitors, tryprostatins A, B and other diketopiperazines produced by aspergillus fumigatus. I. Taxonomy, fermentation, isolation and biological properties. *J. Antibiot.* **49**:534–540 (1996).
14. J. D. Allen, A. Loevezijnvan, J. M. Lakhai, M. Valkvan der, O. Tellingenvan, R. Reid, J. H. Schellens, G. J. Koomen, and A. H. Schinkel. Potent and specific inhibition of the breast cancer resistance protein multidrug transporter *in vitro* and in mouse intestine by a novel analogue of Fumitremorgin C. *Molecular Cancer Therapeutics* **1**:417–425 (2002).
15. J. F. Pouliot, F. L'Heureux, Z. Liu, R. K. Prichard, and E. Gerges. Reversal of P-glycoprotein-associated multidrug resistance by ivermectin. *Biochem. Pharmacol.* **53**:17–25 (1997).
16. D. Schwab, H. Fischer, A. Tabatabaei, S. Poli, and J. Huwyler. Comparison of *in vitro* P-glycoprotein screening assays: recommendations for their use in drug discovery. *J. Med. Chem.* **46**:1716–1725 (2003).
17. A. H. Dantzig, R. L. Shepard, J. Cao, K. L. Law, W. J. Ehlhardt, T. M. Baughman, T. F. Bumol, and J. J. Starling. Reversal of P-glycoprotein-mediated resistance by a potent cyclopropyldibenzosuberane modulator, LY 335979. *Cancer Res.* **56**:4171–4179 (1996).
18. J. H. Lin. Drug–drug interaction mediated by inhibition and induction of P-glycoprotein. *Adv. Drug Deliv. Rev.* **55**:53–81 (2003).
19. C. M. Kruijtzer, J. H. Beijnen, H. Rosing, W. W. ten Bokkel Huinink, M. Schot, R. C. Jewell, E. M. Paul, and J. H. Schellens. Increased oral bioavailability of topotecan in combination with the breast cancer resistance protein and P-glycoprotein inhibitor GF120918. *J. Clin. Oncol.* **20**:2943–2950 (2002).

20. Food and Drug Administration. Drug interaction studies—study design, data analysis, and implications for dosing and labeling (2006). http://www.fda.gov/cder/guidance/6695 dft.pdf (accessed July 17 2007).
21. J. Rautio, J. E. Humphreys, O. W. Lindsey, A. Balakrishnan, J. P. Keogh, J. R. Kunta, C. J. Serabjit-Singh, and J. W. Polli. *In vitro* P-glycoprotein inhibition assays for assessment of clinical drug interaction potential of new drug candidates: a recommendation for probe substrates. *Drug Metab. Dispos.* **34**:786–792 (2006).
22. J. W. Jonker, J. W. Smit, R. F. Brinkhuis, M. Maliepaard, J. H. Beijnen, J. H. Schellens, and A. H. Schinkel. Role of breast cancer resistance protein in the bioavailability and fetal penetration of Topotecan. *J. Natl. Cancer Inst.* **92**:1651–1656 (2000).
23. G. Merino, J. W. Jonker, E. Wagenaar, M. M. Pulido, A. J. Molina, A. I. Alvarez, and A. H. Schinkel. Transport of anthelmintic benzimidazole drugs by breast cancer resistance protein (BCRP/ABCG2). *Drug Metab. Dispos.* **33**:614–618 (2005).
24. P. Breedveld, D. Pluim, G. Cipriani, P. Wielinga, O. Tellingenvan, A. H. Schinkel, and J. H. Schellens. The effect of Bcrp1 (Abcg2) on the *in vivo* pharmacokinetics and brain penetration of imatinib mesylate (Gleevec): implications for the use of breast cancer resistance protein and P-glycoprotein inhibitors to enable the brain penetration of imatinib in patients. *Cancer Res.* **65**:2577–2582 (2005).
25. C. Özvegy, T. Litman, G. Szakács, Z. Nagy, S. Bates, A. Váradi, and B. Sarkadi. Functional characterization of the human Multidrug transporter, ABCG2, expressed in insect cells. *Biochem. Biophys. Res. Commun.* **285**:111–117 (2001).
26. A. Gupta, Y. Zhang, J. D. Unadkat, and Q. Mao. HIV protease inhibitors are inhibitors but not substrates of the human breast cancer resistance protein (BCRP/ABCG2). *J. Pharmacol. Exp. Ther.* **310**:334–341 (2004).
27. R. Evers, M. Kool, A. J. Smith, L. van Deemter, M. de Haas, and P. Borst. Inhibitory effect of the reversal agents V-104, GF 120918, and pluronic L61 on MDR1 P-gp, MRP1- and MRP2- mediated transport. *Br. J. Cancer.* **83**:366–374 (2004).
28. I. J. Hidalgo, T. J. Raub, and R. T. Borchardt. Characterization of the human colon carcinoma cell line (Caco-2) as a model system for intestinal epithelial permeability. *Gastroenterology* **96**:736–749 (1989).
29. J. W. Polli, S. A. Wring, J. E. Humphreys, L. Huang, J. B. Morgan, L. O. Webster, and C. S. Serabjit-Singh. Rational use of *in vitro* P-glycoprotein assays in drug discovery. *J. Pharmacol. Exp. Ther.* **299**:620–628 (2001).
30. C. Özvegy-Laczka, G. Várady, G. Köblös, O. Ujhelly, J. Cervenak, J. D. Schuetz, B. P. Sorrentino, G. Koomen, A. Váradi, K. Német, and B. Sarkadi. Function-dependent conformational changes of the ABCG2 multidrug transporter modify its interaction with a monoclonal antibody on the cell surface. *J. Biochem.* **280**:4219–4227 (2005).
31. R. Clark, I. D. Kerr, and R. Callaghan. Multiple drug binding sites on the R482G isoform of the ABCG2 transporter. *Br. J. Pharmacol.* **149**:506–515 (2006).
32. T. Nakanishi, L. A. Doyle, B. Hassel, Y. Wei, K. S. Bauer, S. Wu, D. W. Pumplin, H. Fang, and D. D. Ross. Functional characterization of human breast cancer resistance protein (BCRP, ABCG2) expressed in the oocytes of *Xenopus laevis*. *Mol. Pharmacol.* **64**:1452–1462 (2003).
33. T. Nakanishi, K. Shiozawa, B. Hassel, and D. D. Ross. Complex interaction of BCRP/ABCG2 and imatinib in BCR-ABL-expressing cells: BCRP-mediated resistance to imatinib is attenuated by imatinib-induced reduction of BCRP expression. *Blood* **108**:678–684 (2006).